



CHORUS

This is the accepted manuscript made available via CHORUS. The article has been published as:

Incomplete protection of the surface Weyl cones of the Kondo insulator SmB_6 : Spin exciton scattering

G. A. Kapilevich, P. S. Riseborough, A. X. Gray, M. Gulacsi, Tomasz Durakiewicz, and J. L. Smith

Phys. Rev. B **92**, 085133 — Published 20 August 2015

DOI: [10.1103/PhysRevB.92.085133](https://doi.org/10.1103/PhysRevB.92.085133)

Incomplete Protection of the Surface Weyl Cones of the Kondo Insulator SmB_6 : Spin Exciton Scattering.

G.A. Kapilevich,¹ P.S. Riseborough,¹ A.X. Gray,¹
M. Gulacsi,² Tomasz Durakiewicz,³ and J.L. Smith³

¹*Temple University, Philadelphia, Pa 19122, USA*

²*Max Planck Institute for the Physics of Complex Systems, Dresden, Germany*

³*Los Alamos National Laboratory, Los Alamos, NM 87545, USA*

Abstract

The compound SmB_6 is a Kondo Insulator, where the lowest-energy bulk electronic excitations are spin-excitons. It also has surface states that are subjected to strong spin-orbit coupling. It has been suggested that SmB_6 is also a topological insulator. Here we show that, despite the absence of time-reversal symmetry breaking and the presence of strong spin-orbit coupling, the chiral spin texture of the Weyl cone is not completely protected. In particular, we show that the spin-exciton mediated scattering produces features in the surface electronic spectrum at energies separated from the surface Fermi energy by the spin-exciton energy. Despite the features being far removed from the surface Fermi energy, they are extremely temperature dependent. The temperature variation occurs over a characteristic scale determined by the dispersion of the spin-exciton. The structures may be observed by electron spectroscopy at low temperatures.

PACS numbers: 78.47. +p, 75.50. Ee, 71.27. +a

I. INTRODUCTION

Heavy-fermion semiconductors, also known as Kondo insulators, are a family of semiconductors with extremely narrow gaps that are subjected to strong electron correlations^{1,2}. The compounds $\text{Ce}_3\text{Bi}_4\text{Pt}_3$, YbB_{12} and SmB_6 can be considered as archetypal members of this class of materials. The Ce-based semiconductors have average occupancies of the atomic 4f electronic shell which are close to unity and, therefore, are close to the Kondo limit. The Ce 4f states are primarily linear superpositions of the non-magnetic $4f^0$ and the moment carrying $4f^1$ states, whereas the Yb-based compounds can be considered as the electron-hole symmetric partners of Ce involving the $4f^{14}$ and $4f^{13}$ configurations. The Sm-based compound SmB_6 is strongly mixed valent and involves the non-magnetic $4f^6$ and the magnetic $4f^5$ configurations that have small term splittings³⁻⁵. The properties of the heavy-fermion semiconducting materials have been described by the Periodic Anderson Model in which the Fermi level resides within the hybridization gap⁶. The strong correlations of Ce or Yb have been incorporated using the slave boson technique appropriate to configurations involving only one 4f electron or one 4f hole.

Since the materials have strong correlations, like most heavy-fermions systems, they can be expected to be close to an instability to a magnetic phase⁷. Therefore, these narrow-gap semiconductors should show magnetic fluctuations that are precursors of transitions to magnetic states⁸⁻¹⁰. This is analogous to the expectation that either paramagnons or antiparamagnons form in paramagnetic metals as precursors to instabilities to ferromagnetic or antiferromagnetic states, respectively. The spin-exciton excitations were first predicted for Ce-based compounds, however, they were observed via inelastic neutron scattering experiments on SmB_6 by Alekseev *et al.*^{11,12} and on YbB_{12} by Bouvet *et al.*^{13,14}. Since the spin-exciton excitations are not seen in the optical conductivity¹⁵, the excitations are not charged and are purely magnetic. The relation of the spin-exciton excitations to quantum criticality has recently been strengthened by their observation in a heavy-fermion semimetal $\text{CeFe}_2\text{Al}_{10}$ ^{16,17}, which is intimately related to the antiferromagnetic system $\text{CeOs}_2\text{Al}_{10}$ ^{18,19}. For SmB_6 , the hybridization gap is of the order of 20 meV, whereas the spin-exciton dispersion relation is in the gap and has a minimum value of about 12 meV at the R point, $\frac{2\pi}{a}(\frac{1}{2}, \frac{1}{2}, \frac{1}{2})$, on the Brillouin zone boundary. Recently, Fuhrman *et al.*²⁰ performed an exten-

sive experimental investigation of the spin-excitons of SmB_6 and found that their dispersion relation has the same periodicity as the Brillouin zone, indicating that the spin-excitons are coherent. Furthermore, they found subsidiary minima in the dispersion relation at the X point $\frac{2\pi}{a}(\frac{1}{2}, 0, 0)$. Fuhrman *et al.* found that the experimentally observed excitations are in excellent agreement with the spin-excitons of an Anderson Lattice Model that has been generalized to include direct 4f to 4f hopping processes.

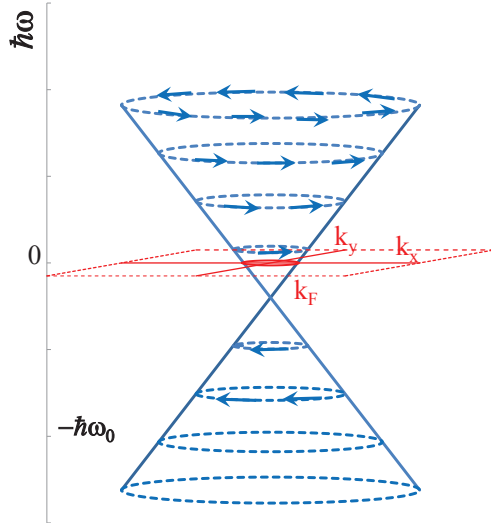


FIG. 1. (Color on line) A sketch of a Weyl cone (blue) over the surface Brillouin zone (red) of SmB_6 . The spin texture is denoted by the arrows. The red circle at $\omega = 0$ depicts the surface Fermi-surface.

Since the resistivity increases with diminishing temperature but plateaus at low temperatures, it has been suggested that SmB_6 has conducting surface states^{21–28}. Like the 4f electrons of all lanthanide elements, the Sm 4f electrons are subject to strong spin-orbit coupling. The surface states are expected to experience a strong Rashba spin-orbit interaction that would lead to the direction of the spins locking to the momenta of the Weyl cones, as sketched in fig.(1). Such spin textures have been observed in non-correlated topological insulators, such as Bi_2Se_3 or $\text{Bi}_{1-x}\text{Sb}_x$ ^{29–31}, and also in SmB_6 ³². It has been suggested that SmB_6 is a topological Kondo insulator^{33–36}. Topological states can result in dissipationless transport and are protected from low-order $\hat{k} \rightarrow -\hat{k}$ scattering by non-magnetic impurities^{37–39}. However, scattering by magnetic impurities⁴⁰ may result in spin-flip scattering, which can result in the reversal of momentum. Apart from the phonons, the spin-exciton excitations

are expected to be the lowest energy bulk excitations of SmB₆. Here, we shall investigate the effect of the scattering of the surface states from the spin-flip scattering of bulk spin-excitons and examine their effect on the states of the Weyl cone.

II. THE SURFACE STATES

We shall describe the surface states by the Rashba Hamiltonian⁴¹

$$H_{S-O} = c \hat{e}_z \cdot \left(\underline{p} \wedge \underline{\sigma} \right) , \quad (1)$$

where c will be the surface Fermi-velocity. Like the spin-orbit coupling for three-dimensional semiconductors, the Rashba coupling for surface states is inversely proportional to the gap. Hence, since the gap Δ in the heavy-fermion semiconductors is extremely small (of the order of 10's of meVs), the Rashba interaction may be expected to be quite large. The Rashba description can be thought of as originating from the Dirac equation in the massless limit, which reduces to two Weyl equations, each of which, separately, breaks inversion symmetry. We shall use the terminology Weyl cone and Weyl point instead of the commonly used terms Dirac cone and Dirac point, since the Dirac cone is gapped except in the massless limit. Also the Dirac energy-eigenvalues are two-fold degenerate corresponding to the two possible values of the helicity, whereas the Weyl equation energy-eigenvalues are singly-degenerate and, therefore, correspond to unique spin textures. The Rashba Hamiltonian can be considered as the reduction of the Hamiltonian of the Weyl equation

$$\left(i \frac{\hbar}{c} \frac{\partial}{\partial t} - \underline{\sigma} \cdot \underline{p} \right) \psi = 0 \quad (2)$$

to two dimensions. This reduction is achieved via the substitution

$$\underline{p} \rightarrow \hat{e}_z \wedge \underline{p} , \quad (3)$$

which eliminates p_z . The eigenstates of the Rashba Hamiltonian forms a Weyl cone which has a chiral spin texture. The eigenstates are found as

$$\phi_{\tau, \underline{k}}(\underline{r}) = \frac{1}{\sqrt{2}} \begin{pmatrix} -\tau \\ \frac{k_y - ik_x}{|\underline{k}|} \end{pmatrix} \exp \left[-i(\omega t - \underline{k} \cdot \underline{r}) \right] , \quad (4)$$

where the energy eigenvalues are $E_\tau(\underline{k}) = \tau \hbar c |\underline{k}|$ and where τ is the chiral index $\tau = \pm 1$. The energy dispersion relations forms a Weyl cone with a vertex at the Weyl point. If

the Fermi level is at an energy other than the Weyl point, one finds a circular surface Fermi-surface ring. The spinorial forms of the eigenstates show that the spin directions reside within the plane of the surface and are locked perpendicular to the directions of the momenta.

In the presence of an applied magnetic field \underline{H} , the spin texture is modified. The external field modifies the dispersion relation is modified to

$$E_\tau(\underline{k}) = \tau \sqrt{\mu_B^2 H_z^2 + (c\hbar k_y + \mu_B H_x)^2 + (c\hbar k_x + \mu_B H_y)^2} . \quad (5)$$

The presence of a magnetic field, aligned with the normal of the surface, gaps the dispersion relation at the Weyl point by introducing a mass term. The gapping of the cone is expected, since the field breaks time-reversal symmetry. For partly-filled bands where the Fermi energy does not either reside in the gap or at the Weyl point, the components of the field perpendicular to the normal of the surface may lead to persistent surface currents circulating round the sample.

Photoemission experiments reveal that there are three Weyl cones in SmB_6 which are centered on the X and the Γ points of the surface Brillouin zone^{25,42-44}. The experiments show that the surface Fermi-surface rings, respectively, have radii of 0.29 and 0.09 \AA^{-1} . Therefore, the Fermi energy does not coincide with the Weyl points. Since the surface Fermi-surface velocities are estimated to be of the order of $300 \sim 220 \text{ meV \AA}^{42,43}$, the extrapolation of the dispersion relations leads to the estimate that the Weyl points reside between 65 and 23 meV below the Fermi energy. Both ARPES and Quantum Oscillation experiments⁴⁵ indicate that the surface Fermi-surface quasiparticles are light, but theories predict heavy quasiparticles^{33-36,46}. This discrepancy could be caused by the neglect of the surface orientation dependence, termination and surface reconstruction⁴⁷ in tight-binding based quasiparticle theories. This discrepancy could also result from a many-body surface instability^{48,49}, such as a Kondo breakdown happening at the surface⁵⁰ where the unbinding of the Kondo singlets gives rise to light quasiparticles. Nevertheless, the tight-binding theories respect the symmetry and topology of the surface states^{33,35,46}. In what follows, we shall consider a single Weyl cone and we shall choose c , the surface Fermi-velocity, such that the surface dispersion relation joins the bands at the surface Brillouin zone boundary, so

$c/a = \frac{\Delta}{4\sqrt{2}}$. Spin-polarized angle resolved photoemission experiments³² show spin textures in which there is an polarization asymmetry in intensity between the lobes at the $+X$ and $-X$ points. The spin texture is a consequence of the Rashba spin-orbit coupling^{51–53}.

III. THE BULK SPIN-EXCITONS

Because the system is both cubic and paramagnetic, the bulk magnetic susceptibility is isotropic in spin space and is given in the RPA by the expression

$$\chi^{\alpha,\alpha}(\underline{q}, \omega) = \frac{\chi^{(0)}(\underline{q}, \omega)}{1 - J \chi^{(0)}(\underline{q}, \omega)} \quad , \quad (6)$$

where J is the effective antiferromagnetic exchange interaction⁵⁴, and $\chi^{(0)}(\underline{q}, \omega)$ is the electron quasiparticle susceptibility, shown in fig.(2) for the electron-hole symmetric case $E_f = 0$, hybridization gap of $V = 0.5 t$ and a tight-binding conduction band of width $6 t$. Due to time-reversal invariance, the real part of $\chi^{(0)}(\underline{q}, \omega)$ is an even function of ω , and the imaginary part is an odd function. The imaginary part of the zero temperature susceptibility at $\underline{Q} = \frac{2\pi}{a}(\frac{1}{2}, \frac{1}{2}, \frac{1}{2})$ is zero within the hybridization gap ($\Delta > |\omega|$). For the parameters chosen here, the gap has a magnitude of $\Delta \sim 2 V^2 / (3 t) \sim t / 6$. The corresponding real part of the susceptibility has a local minimum at $\omega = 0$, and has pronounced peaks near the edges of the particle-hole continuum ($|\omega| \sim \Delta$). As \underline{q} is varied away from \underline{Q} , the magnitude of the real part of the susceptibility near the local minimum at $\omega = 0$ decreases and the range of ω over which the imaginary part of χ^0 is zero increases.

The static, $\omega = 0$, magnetic response function diverges at the wavevector \underline{Q} when

$$1 = J \chi^{(0)}(\underline{Q}, 0) \quad , \quad (7)$$

If $\chi^0(\underline{q}, 0)$ is maximum at wave vector \underline{Q} , then eqn.(7) is the RPA criterion for the minimum value of J for the paramagnetic state to become unstable to a spin density wave state. That is, the resulting divergence of the static susceptibility $\chi^{\alpha,\alpha}(\underline{Q}, 0)$ signals the instability of the system to a static spin-density wave state with wavevector \underline{Q} . Since the real part of $\chi^0(\underline{q}, 0)$ is maximized for wavevectors at the R point $(\frac{1}{2}, \frac{1}{2}, \frac{1}{2})$, the paramagnetic state of the half-filled Anderson Lattice Model shows a tendency to become unstable to a Neel ordered

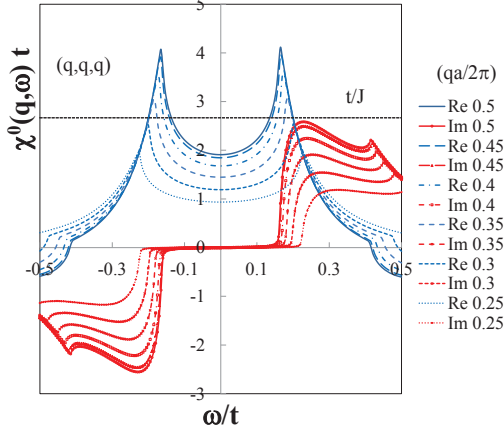


FIG. 2. (Color on line) The dimensionless real (blue lines) and imaginary (red decorated lines) parts of the dynamic quasiparticle susceptibility $\chi^{(0)}(\underline{q}, \omega)$ of the Anderson Lattice Model for various wavevectors \underline{q} . Here, t is the conduction band tight-binding hopping matrix element and the chemical potential μ is within the hybridization gap. The wavevector \underline{q} is directed along the body-diagonal and the q values are shown in the legend.

state.

The dynamic magnetic response function diverges at the frequencies $\omega_{\underline{q}}$ given by the solutions of

$$1 = J \chi^{(0)}(\underline{q}, \omega_{\underline{q}}) \quad (8)$$

which, since the imaginary part of $\chi^{(0)}(\underline{q}, \omega_{\underline{q}})$ is required to vanish, must be outside the electron-hole continuum. The frequencies $\omega_{\underline{q}}$ which satisfy eqn.(8) can be obtained graphically from fig.(2). At each wavevector, the frequency $\omega_{\underline{q}}$ is given by the ω value at which the line J^{-1} intersects with the real part of $\chi^{(0)}(\underline{q}, \omega)$ shown by the blue line and at which the imaginary part of the susceptibility (red decorated lines) is zero. At these real frequencies, the system exhibits persistent staggered magnetic fluctuations, even in the absence of an external time-dependent perturbation. One notes that at a quantum critical point, where eqn.(7) is satisfied, eqn.(8) is automatically satisfied at $\omega_{\underline{Q}} = 0$ which signals the formation of the Goldstone modes of the magnetically ordered state.

The spectrum of magnetic excitations is given by the imaginary part of the susceptibility. Within the gap, the imaginary part of the susceptibility $\chi^{\alpha,\alpha}(\underline{q}, \omega)$ has a delta function

contribution, which is given by

$$\Im \chi^{\alpha,\alpha}(\underline{q}, \omega) = \frac{1}{J} \text{sign}(\omega) \pi \delta\left(1 - J \chi^{(0)}(\underline{q}, \omega)\right) \quad (9)$$

and reduces to

$$\Im \chi^{\alpha,\alpha}(\underline{q}, \omega) = \frac{\text{sign}(\omega)}{Z_{\underline{q}}} \pi \delta(\omega - \omega_{\underline{q}}) . \quad (10)$$

The dimensionless factor $Z_{\underline{q}}$ is defined as a derivative with respect to ω

$$Z_{\underline{q}} = \left| J^2 \left(\frac{\partial}{\partial \omega} \chi^{(0)}(\underline{q}, \omega) \right) \Big|_{\omega=\omega_{\underline{q}}} \right| \quad (11)$$

evaluated at $\omega_{\underline{q}}$. The spin-exciton is a magnetic mode at the frequency $\omega_{\underline{q}}$ in the gap of the two-particle excitation spectrum. The spin-exciton is undamped since there is no available channel for decay into electron-hole pairs.

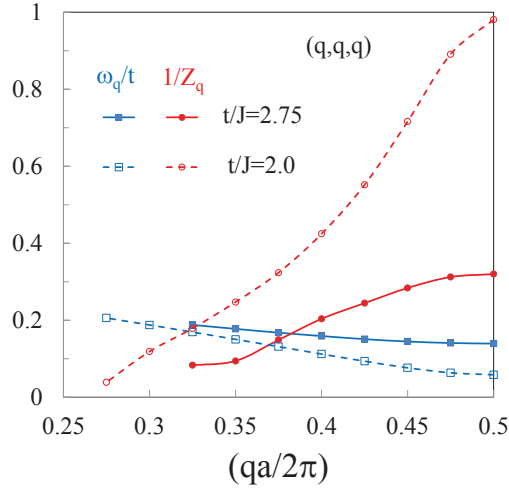


FIG. 3. (Color on line) The dimensionless spin-exciton frequency $\omega_{\underline{q}}$ (blue lines) and its intensity $Z_{\underline{q}}^{-1}$ (red lines) for various wavevectors \underline{q} and two different values of the exchange interaction J . For the value $J = 0.5t$, the spin-exciton energy shows a pronounced minimum at the R point of the Brillouin zone, at which the intensity of the mode approaches unity. For the smaller value of J ($J = 0.36t$), the spin-exciton frequencies are spread over a narrower range and the intensity of the mode shows a weaker dependence on the wavevector.

For the parameters used in fig.(2), the spin-exciton is expected to exist in the paramagnetic semiconductor for values of J in the range $3.2 \Delta > J > 1.5 \Delta$, since J is smaller than

the critical value required for the Neel instability determined by eqn.(7) but large enough to ensure a solution of eqn.(8). For this range of J values, the spin-exciton has a minimum in its dispersion relation at the R point, as is the case for SmB_6 . As \underline{q} is varied away from the R point, the spin-exciton excitation energy increases and eventually merges with the particle-hole continuum, where the mode exists as an overdamped resonance or anti-paramagnon. Hence, the spin-exciton in SmB_6 can be regarded as a precursor excitation for an antiferromagnetic instability that occurs at a nearby quantum critical point in parameter phase space.

Near the quantum critical point, the values of $\omega_{\underline{q}}$ are expected to be low. For small values of $\omega_{\underline{q}}$, the factor $Z_{\underline{q}}$ varies linearly with $\omega_{\underline{q}}$ since $\Re \chi^0(\underline{q}, \omega)$ varies quadratically near $\omega = 0$. Thus, as the spin-exciton mode softens when quantum criticality is approached, its intensity $Z_{\underline{q}}^{-1}$ grows. The dependence of $Z_{\underline{q}}$ on $\omega_{\underline{q}}$ (shown in fig.(3)) is responsible for the peaking of the intensity of the spin-exciton in SmB_6 for momentum transfers \underline{q} near the points $(\frac{1}{2}, \frac{1}{2}, \frac{1}{2})$ and $(\frac{1}{2}, 0, 0)$ where the dispersion relation has minima.

IV. COUPLING OF BULK SPIN-EXCITONS TO SURFACE STATES

The bulk spin-exciton excitations are assumed to couple to the surface states via a Heisenberg exchange interaction

$$\hat{H}_{int} = - \frac{J'}{N} \sum_{\underline{q}, \underline{k}, \sigma, \sigma'} \underline{S}_{-\underline{q}} \cdot \underline{s}_{\sigma, \sigma'} c_{\underline{k}+\underline{q}, \sigma'}^\dagger c_{\underline{k}, \sigma} \quad (12)$$

where \underline{s} is the vector spin operator for the surface electronic states and \underline{S} is the spin-operator which describes the spin excitations of the bulk material. The coupling of the bulk magnetic excitations with the surface electrons has the strength J' . The ratio of the surface to bulk interaction strengths, J'/J , can be quite sizeable, since the characteristic penetration depth of surface states into the bulk is predicted to be of the order of a lattice constant^{36,55}. Using the dispersion relation deduced from photoemission experiments, one estimates that the ratio as

$$\frac{J'}{J} \sim \exp \left[- 2 \frac{\Delta a}{c} \right] \sim 0.576 \quad (13)$$

Recent photoemission experiments provide independent evidence that the surface states may penetrate several lattice spacings into the bulk⁵⁶.

The transformation between the decoupled spin and momentum eigenstates and the Rashba energy eigenstates is given by

$$\begin{aligned}\phi_{\uparrow,\underline{k}}(\underline{r}) &= \frac{1}{\sqrt{2}} \begin{pmatrix} \phi_{-,\underline{k}}(\underline{r}) - \phi_{+,\underline{k}}(\underline{r}) \\ \phi_{\downarrow,\underline{k}}(\underline{r}) = \frac{1}{\sqrt{2}} \begin{pmatrix} \phi_{-,\underline{k}}(\underline{r}) + \phi_{+,\underline{k}}(\underline{r}) \end{pmatrix} \exp[i\varphi_{\underline{k}}\end{pmatrix}\end{aligned}\quad (14)$$

where the phase factor is given by

$$\exp[i\varphi_{\underline{k}}] = \left(\frac{k_y + ik_x}{|\underline{k}|} \right) . \quad (15)$$

The phase $\varphi_{\underline{k}}$ is simply related to the spin orientation of an electron with momentum \underline{k} .

When expressed in terms of the Rashba states, the interaction takes the form

$$\begin{aligned}\hat{H}_{int} = &+ \frac{J'}{4N} \sum_{\underline{q},\underline{k},\tau,\tau'} \left[\tau' \exp[-i\varphi_{\underline{k}+\underline{q}}] S_{-\underline{q}}^+ + \tau S_{-\underline{q}}^- \exp[+i\varphi_{\underline{k}}] \right. \\ &\left. - \left(\tau \tau' - \exp[-i(\varphi_{\underline{k}+\underline{q}} - \varphi_{\underline{k}})] \right) S_{-\underline{q}}^z \right] c_{\underline{k}+\underline{q},\tau}^\dagger c_{\underline{k},\tau'} .\end{aligned}\quad (16)$$

The interaction includes a coupling between the states of the upper and lower parts of the Weyl cone. The coherence factor in front of the $S_{-\underline{q}}^z$ term depends on the relative orientation of the initial and final spin state.

An electron in a surface state with momentum \underline{k} has a self energy due to the emission and absorption of the spin-exciton excitations, which is determined to be

$$\begin{aligned}\Sigma_{\tau}(\underline{k}, \omega) = &\frac{J'^2}{24N} \sum_{\underline{q},\alpha,\tau'} \left[3 - \tau\tau' \cos(\varphi_{\underline{k}-\underline{q}} - \varphi_{\underline{k}}) \right] \int_0^\infty d\omega' \left(\frac{\Im m \chi^{\alpha,\alpha}(\underline{q}, \omega')}{\pi} \right) \\ &\times \left[\frac{1 - f_{\tau',\underline{k}-\underline{q}_{\parallel}} + N(\omega')}{\omega + \mu - E_{\tau'}(\underline{k} - \underline{q}_{\parallel}) - \omega' + i\eta} + \frac{f_{\tau',\underline{k}-\underline{q}_{\parallel}} + N(\omega')}{\omega + \mu - E_{\tau'}(\underline{k} - \underline{q}_{\parallel}) + \omega' - i\eta} \right] ,\end{aligned}\quad (17)$$

where we have assumed that the component of \underline{q} perpendicular to the surface is not conserved. The above expression is related to the self energy due to spin fluctuations in paramagnetic materials close to quantum critical points. The contribution of the in-gap spin-exciton can be simply evaluated by using eqn.(10) and integrating over ω' . This results in the expression

$$\begin{aligned}\Sigma_{\tau}(\underline{k}, \omega) = &\frac{J'^2}{8N} \sum_{\underline{q},\tau'} \frac{1}{Z_{\underline{q}}} \left[3 - \tau\tau' \cos(\varphi_{\underline{k}-\underline{q}} - \varphi_{\underline{k}}) \right] \\ &\times \left[\frac{1 - f_{\tau',\underline{k}-\underline{q}_{\parallel}} + N(\omega_{\underline{q}})}{\omega + \mu - E_{\tau'}(\underline{k} - \underline{q}_{\parallel}) - \omega_{\underline{q}} + i\eta} + \frac{f_{\tau',\underline{k}-\underline{q}_{\parallel}} + N(\omega_{\underline{q}})}{\omega + \mu - E_{\tau'}(\underline{k} - \underline{q}_{\parallel}) + \omega_{\underline{q}} - i\eta} \right] .\end{aligned}\quad (18)$$

Hence, the self energy has an explicit dependence on the square of the ratios of the surface to bulk exchange interactions.

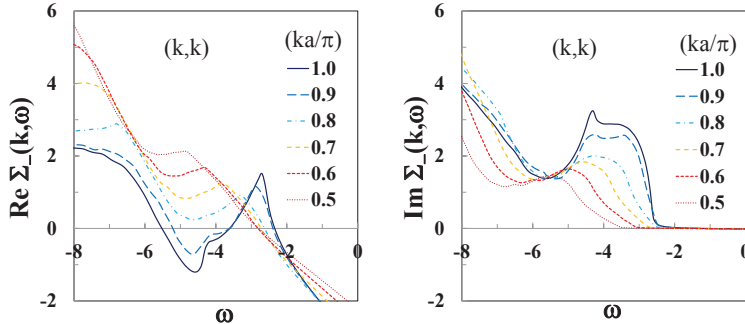


FIG. 4. (Color on line) The frequency dependence of the real (Left Panel) and imaginary parts (Right Panel) of the self energy (in units of meV) for a system close to a bulk Quantum Critical Point, for various wavevectors. The wavevectors \underline{k} are along the diagonal of the surface Brillouin zone and the values of the components are given in the legend in units of $\frac{\pi}{a}$.

We have evaluated the surface one-electron self energy for a system in which the bulk is close to a quantum critical point. The results are shown in fig.(4) for a spin-exciton with a minimum excitation energy of $\omega_0 = 2.5$ meV, $\mu = 2.0$ meV, $\Delta = 20$ meV, $(J'/J)^2 = \frac{\pi}{600}$, and for wavevectors along the diagonal of the surface Brillouin zone. It is seen that the real part of the self energy has a kink near $\omega = -\omega_0$ at which point the imaginary part rapidly increases with decreasing frequency. The self energy has a mild \underline{k} dependence, reflecting a nearly nesting condition, and results in hot patches in the near Fermi energy portions of the Weyl cone.

In the case of a larger value of the minimum spin-exciton energy $\omega_0 = 5.0$ meV, the surface one-electron self energy is almost independent of \underline{q} . The results are shown in fig.(5) for $\mu = 2.0$ meV, $\Delta = 20$ meV, $(J'/J)^2 = \frac{\pi}{600}$, and for wavevectors along the diagonal of the surface Brillouin zone. It is seen that the real part of the self energy has a kink near $\omega = -\omega_0$ at which point the imaginary part abruptly increases with decreasing frequency.

One can find an approximate analytic expression for the self energy of the surface states in the limit of a completely dispersionless spin-exciton by using a continuum model for the

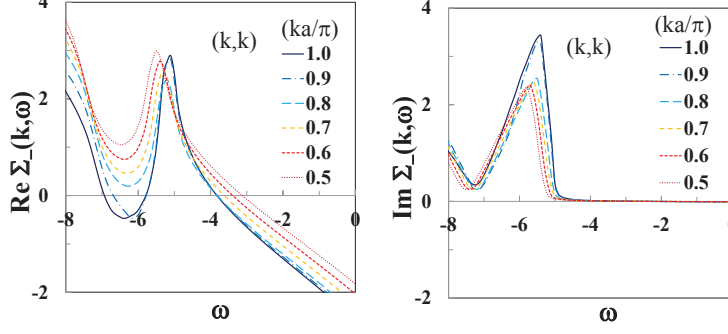


FIG. 5. (Color on line) The frequency dependence of the real (Left Panel) and imaginary parts (Right Panel) of the self energy (in units of meV) for a system close to a bulk Quantum Critical Point, for various wavevectors. The wavevectors \underline{k} are along the diagonal of the surface Brillouin zone and the values of the components are given in the legend in units of $\frac{\pi}{a}$.

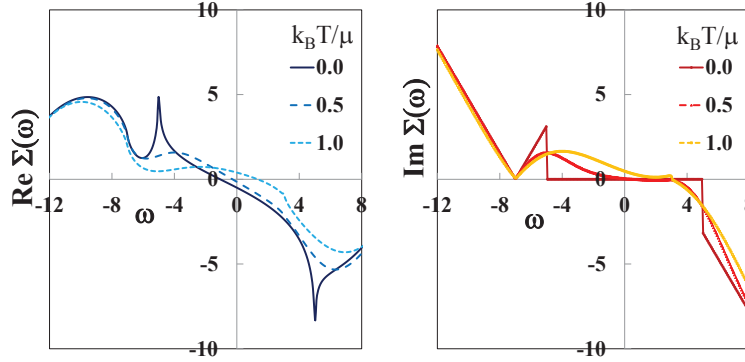


FIG. 6. (Color on line) The real (Left Panel) and imaginary parts (Right Panel) of the self energy at various temperatures (in units of meV) calculated for a flat spin-exciton dispersion relation of $\omega_0 = 5$ meV, and the chemical potential is given by $\mu = 2$ meV. The imaginary parts are denoted by the red lines. The imaginary part of the self energy is zero in the frequency between $+\omega_0$ and $-\omega_0$. The large features in the real part of the self energy at the edges of the frequency range are due to the proximity of the band edges of the cone states. The cusps in the real part of the self energy at $\omega = \pm\omega_0$ are seen to rapidly wash out as T increases.

density of states per surface atom for the Weyl cone. The density of surface states $\rho_0(\epsilon)$, is given by

$$\rho_0(\epsilon) = \frac{\epsilon a^2}{2 \pi c^2} \left[2 \Theta(\epsilon) - \Theta\left(\epsilon - \frac{\Delta}{2}\right) - \Theta\left(\epsilon + \frac{\Delta}{2}\right) \right]. \quad (19)$$

One finds that the real and imaginary parts of the self energies are independent of \underline{k} and,

taking $x_{\pm} = \omega + \mu \pm \omega_0$, can be evaluated at $T = 0$ as

$$\Re \Sigma_{\tau}(\omega) = \left(\frac{3 J'^2 a^2}{16 \pi c^2 Z} \right) \left[x_- \ln \left| \frac{\omega - \omega_0}{x_- - \frac{\Delta}{2}} \right| - x_+ \ln \left| \frac{\omega + \omega_0}{x_+} \right| + x_+ \ln \left| \frac{x_+}{x_+ + \frac{\Delta}{2}} \right| \right]$$

and

$$\Im \Sigma_{\tau}(\omega) = \left(\frac{3 \pi J'^2 a^2}{16 \pi c^2 Z} \right) \left[-x_- \left(\Theta\left(\frac{\Delta}{2} - x_-\right) - \Theta(\omega_0 - \omega) \right) + x_+ \left(\Theta(x_+) - \Theta(\omega + \omega_0) \right) - x_+ \left(\Theta\left(\frac{\Delta}{2} + x_+\right) - \Theta(x_+) \right) \right] . \quad (20)$$

It should be noted that the self-energy is proportional to the inverse square of the surface Fermi-surface velocity. As seen in fig.(6), the resulting quasiparticle scattering rate jumps abruptly at the excitation energy $\omega = -\omega_0$. The magnitude of the jump is determined by the surface density of states at the Fermi energy. The abruptness of the jump is due to our neglect of the dispersion ω_d in the spin-exciton spectrum, and, as seen in fig.(5), for finite ω_d the rapid increase will take place over an energy range given by ω_d . The real part of the self energy shows a sharp cusp in the vicinity of $-\omega_0$.

The electronic spectrum of the surface states is given in terms of the self energy by

$$A_{\tau}(\underline{k}, \omega) = \pm \frac{1}{\pi} \frac{\Im \Sigma_{\tau}(\underline{k}, \omega)}{[\omega + \mu - E_{\tau}(\underline{k}) - \Re \Sigma_{\tau}(\underline{k}, \omega)]^2 + [\Im \Sigma_{\tau}(\underline{k}, \omega)]^2} . \quad (21)$$

The resulting surface quasiparticle density of states is shown in fig.(7), which shows a V-like variation characteristic of the Weyl cone where the density of states goes to zero at the energy of the vertex. However, at the spin-exciton energy, the V-like variation abruptly ceases. The abrupt drop in the spectral density at - 5 meV is primarily due to the divergence in the quasiparticle wave function renormalization

$$Z(\omega) = 1 - \frac{\partial \Sigma(\omega)}{\partial \omega} \quad (22)$$

that occurs at the cusp and is caused by resonant scattering with the spin-excitons. The temperature variation of this feature is not characterized by $\hbar\omega_0$ but is due to the surface electrons in the vicinity of the Fermi energy. The temperature scale is actually set by the dispersion ω_d of the spin-exciton mode.

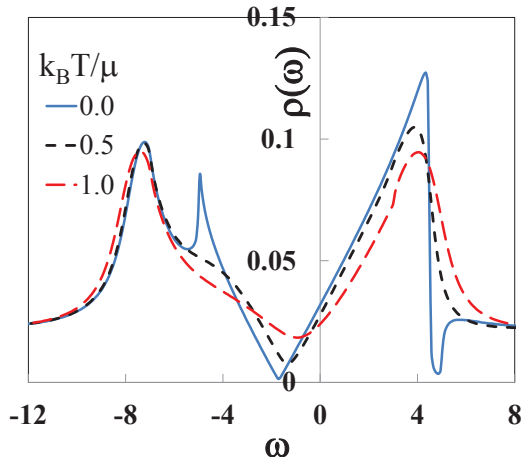


FIG. 7. (Color on line) The calculated angle integrated surface photoemission spectra at various temperatures. The spectrum was calculated for the same parameters as used in fig.(6). The density of states is calculated by assuming that, in addition to the self energy from the emission and absorption of spin-exciton excitations, there is an infinitesimal concentration of magnetic impurities. It is seen that distinct features near $\omega = \pm\omega_0$ rapidly disappear as T is increased.

V. DISCUSSION AND SUMMARY

The above theory predicts a temperature-dependent resonance in the one-electron spectrum at an energy of $\hbar \omega_0$ below the Fermi energy. This temperature-dependent resonance is easily distinguished from the predicted temperature-independent resonance produced by strong elastic scattering from non-magnetic impurities^{39,57}. The energy of the resonance may be markedly reduced from the bulk value since, as has been noted by Alexandrov *et al.*⁵⁰, the characteristic Kondo temperature is expected to be reduced at the surface. In our case, this corresponds to a reduction of the renormalized hybridization gap which pushes the system towards a quantum critical point. This is very similar to the picture envisioned by Doniach⁷ for three-dimensional heavy-fermion metals where, for a sufficiently large magnetic degeneracy, a reduction in the Kondo temperature may result in an antiferromagnetic instability. For systems with the right symmetry, the antiferromagnetic phase may also be topologically protected despite the breaking of time-reversal invariance⁵⁸. Within our picture, the instability would occur via a condensation of spin-excitons forming an antiferromagnetic surface state. Our picture is to be contrasted with the picture of Alexandrov *et al.*⁵⁰ in which the surface Kondo singlets would unbind at the quantum critical point.

Here, we examined the effect of the precritical antiferromagnetic fluctuations of the bulk insulating state on the metallic surface states. Our analysis is predicated on the value of J'/J being sizeable, which implies that the surface states penetrate several unit cells into the bulk. As argued in ref.³⁶, a sizeable penetration depth requires that the ratio of c to Δ be of the order of a . The required ratio is consistent with the large velocities inferred from ARPES measurements^{42,43}. However, the value of the ratio c/Δ is incompatible with the surface-bulk correspondence which requires a smaller value of c and, therefore, produces a smaller J'/J ratio. However, the decrease in the ratio of J'/J is partially offset by the decrease in surface Fermi-velocity, since the self energy is explicitly proportional to a factor of $\left(\frac{J'}{Jc}\right)^2$. This trend is in accord with the observation of Triola *et al.*⁴⁹ that heavy surface quasiparticle masses promote many-body effects and instabilities.

In summary, the Weyl cones in a strongly correlated Kondo insulator, in which there are low-energy spin-exciton excitations, are neither protected by symmetry nor by the spin-orbit coupling despite the absence of broken time-reversal symmetry. We have found that at zero temperature, the imaginary part of the self energy exhibits a non-analytic behavior at the spin-exciton energy. The non-analytic behavior is a reflection of the non-analytic behavior of the unrenormalized density of states of the Weyl cone. The non-analytic behavior of the imaginary part of the self energy leads to an anomaly in the dispersion relation of the surface quasiparticles states that is responsible for structure in the electronic spectrum. Although this feature is at ω_0 and is far removed from the surface Fermi energy, it is extremely temperature dependent and washes out rapidly as the temperature is increased. The rapid temperature dependence originates from a virtual process that involves states right at the surface Fermi energy, and the temperature scale is set by the dispersion in the spin-exciton energy. The spin-exciton induced structure in the surface electronic spectrum may be measured by high-resolution ARPES measurements or by tunneling experiments at low temperatures.

VI. ACKNOWLEDGEMENTS.

The work at Temple was supported by an award from the US Department of Energy, Office of Basic Energy Sciences, via the award DE-FG02-01ER45872. PSR would like to acknowledge stimulating conversations with Pedro Schlottman, Collin Broholm, Wes Fuhrman, Laura Greene and Wan-Kyu Park. TD acknowledges the NSF IR/D program.

-
- ¹ G. Aeppli and Z. Fisk, *Comm. Cond. Mat. Phys.* **16**, 155 (1992).
 - ² P.S. Riseborough, *Adv. in Phys.* **49**, 257 (2000).
 - ³ A. Menth, E. Buehler and T.H. Geballe, *Phys. Rev. Lett.* **22**, 295-298 (1969).
 - ⁴ J.C. Nickerson, R.M. White, K.N. Lee, R. Bachman, T.H. Geballe and G.W. Hull Jr., *Phys. Rev. B*, **3**, 2030-2042 (1971).
 - ⁵ R.M. Martin and J. Allen, *J. Appl. Phys.* **50**, 7561 (1979).
 - ⁶ P.S. Riseborough, *Phys. Rev. B*, **45**, 13984 (1992).
 - ⁷ S. Doniach, *Physica B & C*, **91**, 231-234 (1977).
 - ⁸ P.S. Riseborough, *Annalen der Physik*, **9**, 813-820 (2000).
 - ⁹ P.S. Riseborough, *J. Mag. Mag. Mat.* **226**, 127-128 (2001).
 - ¹⁰ P.S. Riseborough, *Phys. Rev. B*, **68**, 235213 (2003).
 - ¹¹ P.A. Alekseev, J.-M. Mignot, J. Rossat-Mignod, V.N. Lazukov, I.P. Sadikov, E.S. Konalova and Y.B. Paderno, *J. Phys. Cond. Mat.* **7**, 289 (1995).
 - ¹² P.A. Alekseev, V.N. Lazukov, K.S. Nemovskii and I.P. Sadikov, *J. Exp. Theor. Phys.* **111**, 285 (2010).
 - ¹³ A. Bouvet, T. Kasuya, M. Bonnet, L.P. Regnault, J. Rossat-Mignod, F. Iga, B. Fak and A. Severing, *J. Phys. Cond. Mat.* **10**, 5667-5677 (1998).
 - ¹⁴ F. Iga, A. Bouvet, L.P. Regnault, T. Takabatake, A. Hiess and T. Kasuya, *J. Phys. Chem. Solids*, **60**, 1193-1196 (1999).
 - ¹⁵ B. Gorshunov, N. Sluchanko, A. Volkov, M. Dressel, G. Knebel, A. Loidl, and S. Kunii, *Phys. Rev. B*, **59**, 1808 (1999).

- ¹⁶ J.M. Mignot, P.A. Alekseev, J. Robert, S. Petit, T. Nishioka, M. Matsumura, R. Kobayashi, H. Tanida, H. Nohara and M. Sera, Phys. Rev. B, **89**, 161103 (2014).
- ¹⁷ D.T. Adroja, A.D. Hillier, Y. Muro, J. Kajino, T. Takabatake, P. Peratheepan, A.M. Strydom, P.P. Deen, F. Demmel, J.R. Stewart, J. W. Taylor, R.I. Smith, S. Ramos and M.A. Adams, Phys. Rev. B, **87**, 224415 (2013).
- ¹⁸ Y. Muro, J. Kajino, K. Umeo, K. Nishimoto, R. Tamura and T. Takabatake, Phys. Rev. B, **81**, 214401 (2010).
- ¹⁹ D. T. Adroja, A. D. Hillier, P. P. Deen, A. M. Strydom, Y. Muro, J. Kajino, W. A. Kockelmann, T. Takabatake, V. K. Anand, J. R. Stewart and J. Taylor, Phys. Rev. B, **82**, 104405 (2010).
- ²⁰ W.T. Fuhrman, J. Leiner, P. Nikolic, G.E. Granroth, M.B. Stone, M.D. Lumsden, L. DeBeer-Schmidt, P.A. Alekseev, J.-M. Mignot, S.M. Koopayeh, P. Cottingham, W.A. Phelam, L. Schloop, T.M. McQueen and C. Broholm, Phys. Rev. Lett. **114**, 036401 (2015).
- ²¹ D.J. Kim, T. Grant and Z. Fisk, Phys. Rev. Lett. **109**, 096601 (2012).
- ²² D.J. Kim, S. S. Thomas, T. Grant, J. Botimer, Z. Fisk and J. Xia, Sci. Reps. **3**, 3150 (2013).
- ²³ X. Zhang, N.P. Butch, P. Syers, S. Ziemak, R.L. Greene and J.P. Paglione, Phys. Rev. X, **3**, 011011 (2013).
- ²⁴ S. Wolgast, Ç. Kurdak, K. Sun, J. W. Allen, D.-J. Kim, and Z. Fisk, Phys. Rev. B **88**, 180405(R) (2013).
- ²⁵ N. Xu, X. Shi, C.E. Matt, R.S. Dhaka, Y. Huang, N.C. Plumb, M. Radović, J.H. Dil, E. Pomjakushima, K. Conder, A. Amato, Z. Salman, D. McK. Paul, J. Mesot, H. Ding and M. Shi, Phys. Rev. B, **88**, 121102 (2013).
- ²⁶ D.J. Kim, J. Xia, and Z. Fisk, Nat. Mater. **13**, 466 (2014).
- ²⁷ J. Yong, Y. Jiang, D. Usanmaz, S. Curtarolo, X. Zhang, L. Li, X. Pan, J. Shin, I. Takeuchi and R.L. Greene, App. Phys. Lett. **105**, 222403 (2014).
- ²⁸ P. Syers, D. Kim, M.S. Fuhrer and J-P. Paglione, Phys. Rev. Lett. **114**, 096601 (2015).
- ²⁹ Y. Xia, D. Qian, D. Hsieh, L. Wray, A. Pal, H. Lin, A. Bansil, D. Grauer, Y.S. Hor, R.J. Cava, and M.Z. Hasan, Nat. Phys. **5**, 398-402 (2009).
- ³⁰ D. Hsieh, Y. Xia, D. Qian, L. Wray, D. Qian, F. Meier, J.H. Dil, J. Osterwalder, L. Patthey, A.V. Fedorov, A. Bansil, D. Grauer, Y.S. Hor, R.J. Cava and M.Z. Hasan, Phys. Rev. Lett. **103**, 14640 (2009).

- ³¹ D. Hsieh, Y. Xia, L. Wray, D. Qian, A. Pal, J.H. Dil, J. Osterwalder, F. Meier, G. Bihlmayer, C.L. Kane, Y.S. Hor, R.J. Cava and M.Z. Hasan, *Science*, **323**, 919-922 (2009).
- ³² N. Xu, P.K. Biswas, J.H. Dil, R.S. Dhaka, G. Landolt, S. Muff, C.E. Matt, X. Shi, N.C. Plumb, M. Radović, E. Pomjakushina, K. Conder, A. Amato, S.V. Borisenko, R. Yu, H.-M. Weng, Z. Fang, X. Dai, J. Mesot, H. Ding and M. Shi, *Nature Commun.* **5**, 4566 (2014).
- ³³ M. Dzero, K. Sun, V. Galitski and P. Coleman, *Phys. Rev. Lett.*, **104**, 106408 (2010)
- ³⁴ M. Dzero, K. Sun, P. Coleman and V. Galitski, *Phys. Rev. B*, **85**, 045130 (2012).
- ³⁵ T. Takimoto, *J. Phys. Soc. Japan*, **80**, 123710 (2011).
- ³⁶ V. Alexandrov, M. Dzero and P. Coleman, *Phys. Rev. Lett.* **111**, 226403 (2013).
- ³⁷ W.-C. Lee, C. Wu, D. Arovas and S.-C. Zhang, *Phys. Rev. B*, **80**, 245349 (2009).
- ³⁸ X. Zhou, C. Fang, W.-F. Tsai and J.-P. Hu, *Phys. Rev. B*, **80**, 245317 (2009).
- ³⁹ R.R. Biswas and A.V. Balatsky, *Phys. Rev. B*, **81**, 233405 (2010).
- ⁴⁰ G.-Z. Liu, W. Lee and G. Cheng, *Phys. Rev. B*, **79**, 205429 (2009).
- ⁴¹ E.I. Rashba, *Sov. Phys. Solid State*, **2**, 1109 (1960).
- ⁴² M. Neupane, N. Alidoust, S.-Y. Xu, T. Kondo, D.-J. Kim, C. Liu, T.-R. Chang, H.-T. Jeng, T. Durakiewicz, L. Balicas, H. Lin, A. Bansil, S. Shin, Z. Fisk and M.Z. Hasan, *Nature Commun.* **4**, 2991 (2013).
- ⁴³ J. Jiang, S. Li, T. Zhang, Z. Sun, F. Chen, Z.R. Ye, M. Xu, Q.Q. Ge, S.Y. Tan, X.H. Niu, M. Xia, B.P. Xie, X.H. Chen, H.H. Wen and D.L. Feng, *Nature Commun.* **4**, 3010 (2013).
- ⁴⁴ E. Frantzeskakis, N. de Jong, B. Zwartsenberg, Y.K. Huang, Y. Pan, X. Zhang, J.X. Zhang, F.X. Zhang, L.H. Bao, O. Tegus, A. Varykhalov, A. de Visser and M.S. Golden, *Phys. Rev. X*, **3**, 041024 (2013).
- ⁴⁵ G. Li, Z. Xiang, F. Yu, T. Asaba, B. Lawson, P. Cai, C. Tinsman, A. Berkley, S. Wolgast, Y. S. Eo, D.-J. Kim, Ç. Kurdak, J.W. Allen, K. Sun, X. H. Chen, Y. Y. Wang, Z. Fisk and L. Li, *Science*, **346**, 1208-1212 (2014).
- ⁴⁶ F. Lu, J-Z. Zhao, H. Weng, Z. Fang and Xi Dai, *Phys. Rev. Lett.* **110**, 096401 (2013).
- ⁴⁷ S. Rössler, T-H. Jang, D-J. Kim, L.H. Tjeng, Z. Fisk, F. Steglich and S. Wirth, *Proc. Nat. Acad. Sci. USA*, **111**, 4798-4802 (2014).
- ⁴⁸ P. Nikolic, *Phys. Rev. B*, **90**, 235107 (2014).
- ⁴⁹ C. Triola, J-X. Zhu, A. Migliori, A.V. Balatsky, arXiv:1501.03158 (2015).
- ⁵⁰ V. Alexandrov, P. Coleman and O. Erten, *Phys. Rev. Lett.* **114**, 177202 (2015).

- ⁵¹ P.P. Baruselli and M. Vojta, Phys. Rev. B, **90**, 2011106 (2014).
- ⁵² M. Legner, A. Rüegg and M. Sigrist, Phys. Rev. B, **90**, 085110 (2014).
- ⁵³ R. Yu, H. Weng, X. Hu, Z. Fang and X. Dai, New J. Phys. **17**, 023012, (2015).
- ⁵⁴ S. Doniach, Phys. Rev. B, **35**, 1814-1821 (1987).
- ⁵⁵ P. Schlottmann, Phys. Rev. B. **90**, 165127 (2014).
- ⁵⁶ P. Hlawenka, K. Siemensmeyer, E. Weschke, A. Varykhalov, J. Sanchez-Barriga, N.Y. Shit-selova, A.V. Dukhenko, V.B. Fillipov, S. Gabani, K. Flachbart, O. Rader and E.D.L. Rienks, <http://arxiv.org/abs/1502.0154> (2015).
- ⁵⁷ A.M. Black-Schaffer, A.V. Balatsky and J. A. Fransson, Phys. Rev. B, **91**, 201411 (2015).
- ⁵⁸ R.S.K. Mong, A.M. Essin and J.E. Moore, Phys. Rev. B **81**, 245209 (2010).